

# Fabrication of Bimodal Porous Silicate with Silicalite-1 Core/Mesoporous Shell Structures and Synthesis of Nonspherical Carbon and Silica Nanocases with Hollow Core/Mesoporous Shell Structures

Jong-Sung Yu,<sup>\*,†</sup> Suk Bon Yoon,<sup>†</sup> Yun Jo Lee,<sup>‡</sup> and Kyung Byung Yoon<sup>‡</sup>

Department of Chemistry, Hannam University, Daejeon, 306-791, Republic of Korea, and  
Center for Microcrystal Assembly and Department of Chemistry, Sogang University,  
Seoul, 121-742, Republic of Korea

Received: November 18, 2004; In Final Form: January 26, 2005

In this work, an attempt has been made to modify the shape and nanostructure of core–shell materials, which have been usually generated on the basis of amorphous spherical cores. Novel core–shell silicate particles, each of which consists of a silicalite-1 zeolite crystal core and mesoporous shell (ZCMS), were synthesized for the first time. The ZCMS core–shell particles are unique because they are of pseudohexagonal prismatic shape and have hierarchical porosity of both a uniform microporous core and a mesoporous shell coexisting in a particle framework. The nonspherical bimodal porous core–shell particles were then utilized as templates to fabricate a new carbon replica structure. Interestingly, the pore replication process was carried out only through the mesopores in the shell, and not through the micropores due to the narrower micropore size in the core, resulting in nonspherical carbon nanocases with a hollow core and mesoporous shell (HCMS) structure. Nonspherical silica nanocases with HCMS structure were also generated by replication using the carbon nanocases as templates, which are not possible to synthesize through other synthetic methods. Interestingly, the pseudohexagonal prismatic shape of the zeolite crystals was transferred onto the carbon and silica nanocases.

## Introduction

The synthesis of new nanostructured materials with tailored porosity is a major challenge in advanced materials science. Nanoporous materials such as zeolites and mesoporous molecular sieves have been widely used in various applications including catalysis, adsorption, and separation processes due to their well-developed ordered porous structures with high specific surface area, large pore volume, and narrow pore size distribution.<sup>1</sup> Amine molecules or surfactant micelles have been used to template the synthesis of these nanoporous materials. These porous materials, in turn, provide new opportunities as scaffolds for the templated fabrication of new novel nanostructured materials.<sup>2–4</sup> Nanostructured carbon materials were prepared by chemical vapor deposition (CVD) and/or impregnation method using various types of zeolites as templates.<sup>2</sup> The nanocasting of mesoporous carbons and polymers has been reported with the use of mesoporous molecular sieves, MCM-48, and SBA-15 as templates.<sup>3,4</sup> Various colloidal crystals based on the ordered aggregation of spherical nanoparticles such as silica and latex polymer spheres also have been employed for template synthesis of new uniform macroporous materials including polymers,<sup>5</sup> inorganic oxides,<sup>6</sup> metals,<sup>7</sup> carbons,<sup>8</sup> and SiC.<sup>9</sup>

Colloidal templating has been also extensively explored as an efficient route to the production of various core–shell or hollow capsule structures. Many new nanostructured shell frameworks with either solid core or hollow core were generated depending on the removal of core templates. Considerable interest in these materials stems from their various potential

applications as catalytic supports, packing materials for separations, and small containers for encapsulation.<sup>10–13</sup> Most colloidal templating approaches for the generation of such core–shell or hollow capsule type structures have been performed exclusively with amorphous spherical particles as core materials. Various types of nanostructures have been explored from compositions such as inorganic materials,<sup>10</sup> polymers,<sup>11</sup> and carbon,<sup>12</sup> and composites<sup>13</sup> for the shell. However, there are very few reports on modification of the core shape beyond the common spherical shape.<sup>10f,11b</sup> In addition, very little attention has been paid to the core nanostructure. It would be more challenging to create new core–shell materials through modifying the core structure by replacing an amorphous spherical core with a nanostructured nonspherical core. Various molecular sieve zeolites crystallize with distinct morphological shapes such as cubic, octahedral, and prismatic shapes.<sup>14</sup> Thus, by employing zeolite crystals with particular shapes as core materials, not only the shape but also the nanostructures of the core–shell materials will be modulated at a controllable level. To the best of our knowledge, there has been no report on the synthesis of microporous zeolite core crystals covered with thin mesoporous shells of even thickness. In this work, we report the first synthesis of bimodal porous silicate with a zeolite core/mesoporous shell (ZCMS) structure consisting of a nonspherical zeolite silicalite-1 core crystal particle and surrounding mesoporous shell, and the fabrication of nonspherical pseudohexagonal prismatic carbon and silica nanocases with hollow core/mesoporous shell (HCMS) structures by employing the ZCMS silicate as a template.

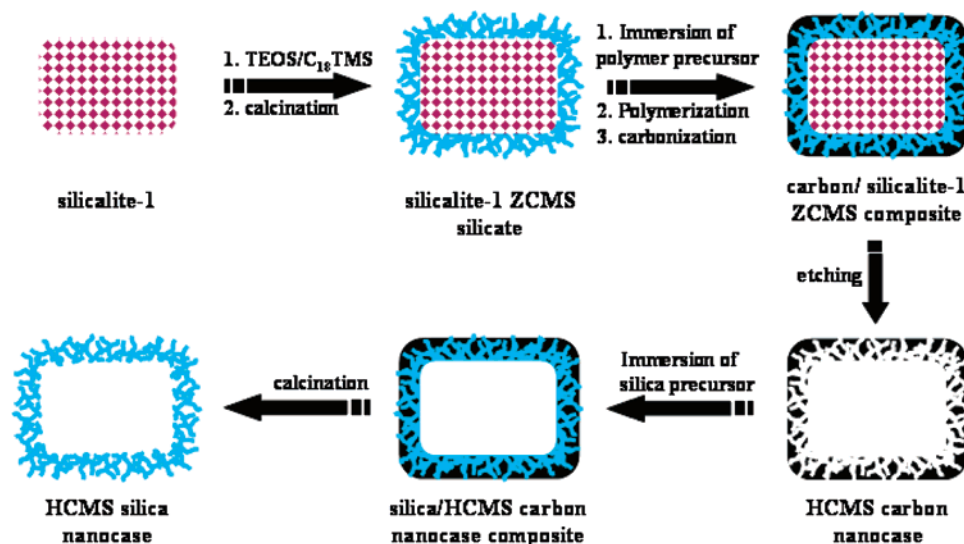
## Experimental Procedures

**Synthesis of Silicalite-1 Zeolite Core/Mesoporous Shell Aluminosilicate Templates.** Pseudohexagonal prismatic zeolite

\* To whom correspondence should be addressed. Phone: +82-42-629-7446. Fax: +82-42-629-7444. E-mail: jsyu@hannam.ac.kr.

<sup>†</sup> Hannam University.

<sup>‡</sup> Sogang University.

**SCHEME 1:** Schematic Illustration for Synthesis of Silicalite-1 ZCMS Core–Shell Particles and Corresponding Pseudo-hexagonal Prismatic HCMS Carbon and Silica Nanocases

particles with MFI structure were synthesized according to literature procedures.<sup>15</sup> The MFI structure synthesized in this work is of pure silica form and is typically called silicalite-1. To fabricate the ZCMS core–shell silicate particles, 8 mL of aqueous ammonia (28 wt %) was added to a solution containing 200 mL of absolute ethanol and 16 mL of deionized water. Then 2.0 g of the calcined silicalite-1 was added to the above-prepared mixture. Extra caution was used in handling the silicalite-1 particles because they easily tend to stick together in solution. Right after mixing calcined silicalite-1 with the solution, the reaction mixture was sonicated for 1 h and subsequently stirred for 30 min in order to set the silicalite-1 particles as far apart as possible. A mixture solution containing 0.7–2.5 mL of TEOS and 0.5 mL of octadecyltrimethoxysilane ( $C_{18}$ -TMS) (with molar ratios of  $TEOS/C_{18}$ -TMS = 2.6–9.3) was then added to the reaction mixture bottles under vigorous stirring and subsequently stirred at ambient temperature for 6 h. As-synthesized octadecyl group incorporated ZCMS core–shell silicate particles were retrieved by centrifugation, and were further calcined at 823 K for 6 h in air to remove octadecyl groups in the mesoporous shell. Aluminum was incorporated into the ZCMS framework via an impregnation method to yield ZCMS aluminosilicate with strong acid sites for the polymerization of phenol and paraformaldehyde.<sup>16</sup>

**Synthesis of Pseudo-hexagonal Prismatic Carbon Nanocases.** Into 1.0 g of evacuated silicalite-1 ZCMS aluminosilicate template was 0.174 g of phenol incorporated by heating at 373 K for 12 h under static vacuum. The resulting phenol-incorporated ZCMS silicates were then reacted with 0.141 g of paraformaldehyde under static vacuum at 403 K for 24 h to yield in situ polymerized phenolic resin–ZCMS composite. The composite was placed in the tube furnace and then heated at 1 K  $min^{-1}$  to 433 K and held at that temperature for 5 h under flowing nitrogen. The temperature was then ramped at 5 K  $min^{-1}$  to 1273 K and held at that temperature for 7 h to carbonize the resin in the ZCMS templates in order to finally get a carbon–ZCMS composite. Dissolution of the ZCMS silicate by dilute HF solution generated carbon nanocases with HCMS structure.

**Synthesis of Pseudo-hexagonal Prismatic Silica Nanocases.** HCMS carbon nanocases were filled with TEOS as silica precursor, and subsequently the excess silica precursor was removed by vacuum evaporation. Infiltration of the mesopores

with TEOS was exercised under static vacuum. The silica precursor–HCMS carbon nanocase composite was exposed to HCl vapor to induce hydrolysis and condensation of the silica precursor in a sealed reaction bottle at 373 K overnight. Finally, the silica–HCMS carbon nanocase composite was heated at 823 K for 7 h in air to remove the carbon framework.

**Characterization.** Powder X-ray diffraction (XRD) measurements were taken with a Rigaku D/MAX-III (3 kW) with Cu  $K\alpha$  radiation at a scan rate of 4°/min. The nitrogen adsorption and desorption isotherms were measured at 77 K using a Micromeritics ASAP 2010 system. Surface areas and pore volumes were determined by nitrogen adsorption data in the relative pressure range from 0.05 to 0.2 using the BET equation. Total pore volume was measured at  $P/P_0 = 0.98$ . The pore size distribution curve was obtained from the analysis of the adsorption branch of the nitrogen isotherm using the BJH (Barrett–Joyner–Halenda) method.<sup>17</sup> Surface morphologies of the porous carbons were examined by a scanning electron microscope (SEM, LEO 1455VP, Hitach S-4700) operated at an acceleration voltage of 25 kV. The microscopic features of the sample were observed with a transmission electron microscope (TEM, EM 912 Omega) operated at 200 kV.

## Results and Discussion

The overall synthetic procedure is shown in Scheme 1. Monodisperse pseudo-hexagonal prismatic silicalite-1 particles were synthesized by a reported method.<sup>15</sup> Mesoporous shell layer was fabricated by cohydrolysis and subsequent sol–gel condensation of TEOS and  $C_{18}$ -TMS on each silicalite-1 particle followed by the removal of the octadecyl organic group.<sup>10a,12</sup> The best synthesis was performed by employing molar ratios of  $TEOS/C_{18}$ -TMS = 5.5–4.5.  $C_{18}$ -TMS has a function of a porogen to generate the porosity in the shell. Figure 1 shows the scanning electron microscopic (SEM) and the transmission electron microscopic (TEM) images for the silicalite-1 ZCMS core–shell composite silicate particles. The silicalite-1 particles have a nearly monodisperse pseudo-hexagonal prismatic shape with an average size of  $\sim 1.0 \times 0.8 \times 0.43 \mu m$ . The mesoporous shell was evenly formed with roughly uniform thickness of about 40 nm over each of the silicalite-1 crystals, maintaining the overall shape of the silicalite-1 crystal as shown in the figure. The mesopores in the shell are clearly seen in the TEM image

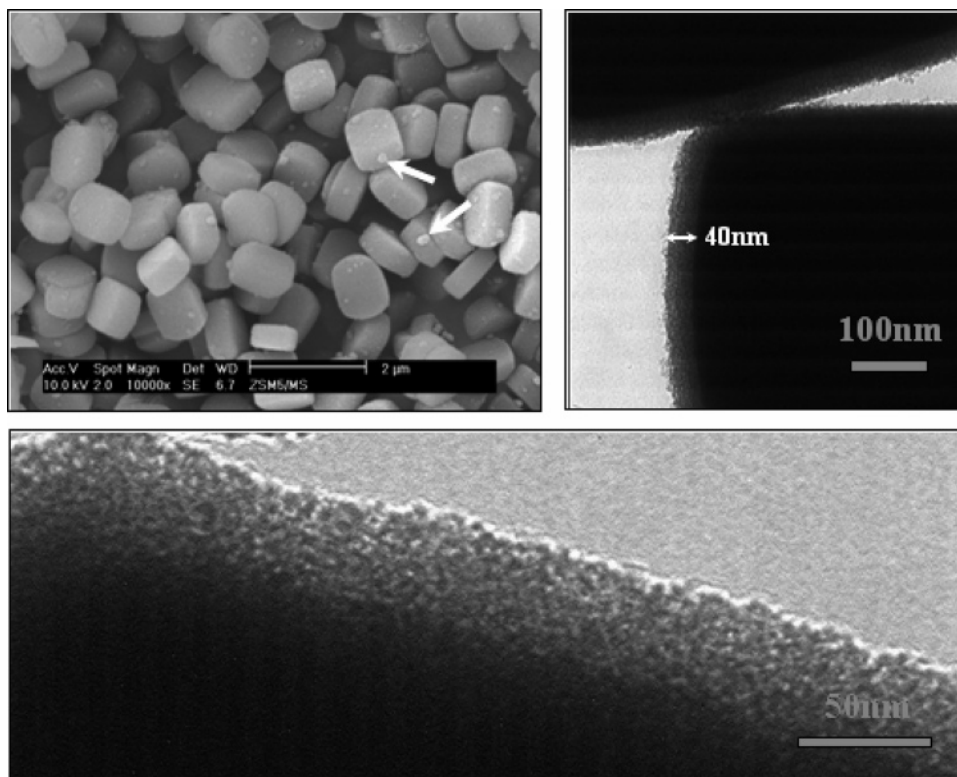


**Figure 1.** Scanning electron microscope (SEM) (top left) and transmission electron microscope (TEM) (top right) images for silicalite-1 ZCMS core-shell particles. TEM image at high magnification of the ZCMS shell (bottom).

at high magnification. In this case, the shells have a three-dimensionally interconnected randomly distributed mesopore arrangement unlike the ordered mesopore arrangement found in hexagonal MCM-41 type silica.<sup>1b,12</sup> This is the first synthesis of the core-shell silicate particles, each of which is composed of a silicalite-1 zeolite crystal core and surrounding mesoporous silica shell, and represents one step forward in the synthesis of core-shell type materials by using nonspherical pseudo-hexagonal prismatic nanostructured zeolite crystals instead of the usual amorphous spherical particles used in previous works.<sup>10–13</sup> In addition, since micropores and mesopores are generated by their respective different synthetic approaches, these two different pore types cannot coexist in a framework. Although several interesting materials have been reported, in which both macropores and micro- or mesopores are incorporated into a structure, these are not core-shell types.<sup>18</sup> Thus, the ZCMS particles represent a unique and novel nanostructured system in that each individual particle has a core-shell type bimodal pore system of both micropores and mesopores in a particle. These silicalite-1 ZCMS particles can find potential applications as size-selective multifunctional catalytic materials and chromatographic separation materials. Small silica particles, which are believed to be formed as side products during the synthesis of the mesoporous shell over the silicalite-1 core particles, are occasionally seen on the surface of the core-shell particles as indicated by arrows in the SEM image.

Figure 2 shows SEM and TEM images of the nonspherical carbon and silica nanocases with HCMS structures, which were fabricated by using silicalite-1 ZCMS silicates as templates and in situ preformed phenolic resin as the carbon source.<sup>12</sup> In the synthesis, the sacrificial porous ZCMS silica molds were infiltrated with carbon precursor, which is subsequently carbonized under nonoxidizing conditions, and then removed by dissolving in HF or NaOH solution to generate porous carbons. During the replication process the pores and walls of the host

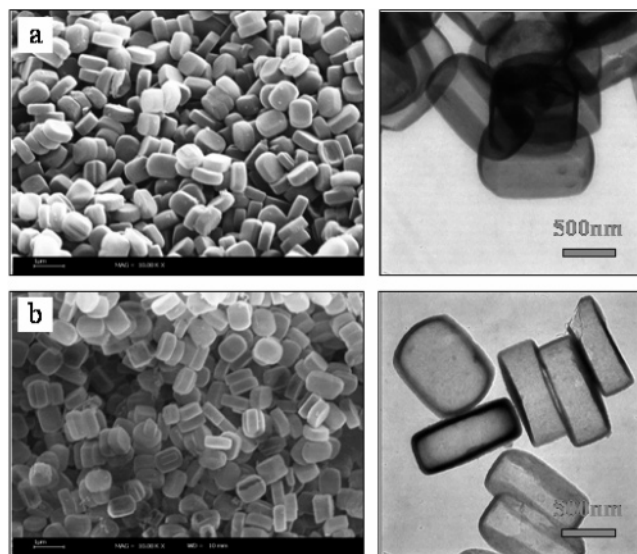


**Figure 2.** Scanning electron microscope (SEM) (left) and transmission electron microscope (TEM) (right) images for pseudo-hexagonal prismatic (a) carbon nanocases and (b) silica nanocases with HCMS structures.

were transformed to the walls and pores, respectively, of the resulting carbon framework. Thus the host scaffold materials are required to have interconnected pore systems, which allow for structural integrity of the templated carbon after removal of the host. It is interesting to note that the resulting carbon structures bear the shape of the original silicalite-1 crystals, showing a uniform pseudo-hexagonal prismatic shape. The SEM image reveals a hollow core inside broken particles. TEM clearly shows hollow cores with mesoporous shells of even thickness in the particles. This indicates that a carbon layer was generated only in the mesoporous shell part of the silicalite-1 ZCMS particles. The micropores in silicalite-1 particles may be too



small for the polymer precursors to enter. Silicalite-1 structure comprises interconnecting straight ( $0.56 \times 0.53$  nm) and sinusoidal channels ( $0.51 \times 0.55$  nm).<sup>19</sup> Thus, the largest channel size is about 0.56 nm, which is smaller than phenol with the kinetic diameter of  $\sim 0.6$  nm.<sup>20</sup> Although phenol is slightly bigger than the channel sizes, some phenol might enter the channels, as shown in the formation of coordination complexes observed between phenol and Cu(II) ion exchanged into the silicalite-1 framework, which were monitored by electron spin resonance spectra,<sup>21</sup> but not to such an extent that they can form in situ polymerized resin. Thus polymerization and subsequent carbonization should occur only on the mesoporous shell region. This is consistent with earlier reports,<sup>2a,e</sup> in which carbon deposition took place mostly on the external surface of silicalite-1 particles in the synthesis of the carbon replica employing furfuryl alcohol as carbon precursor.

The carbon capsules with HCMS structures can also provide an incentive for the synthesis of new novel nanoporous inorganic materials. Back replication using the carbon nanocases as templates and through the sol–gel process of a silica source can result in new silica structures.<sup>21</sup> Figure 2b shows the SEM and TEM images for silica nanocases retrieved after removal of the carbon nanocase templates. The silica nanocases possessed the same nonspherical pseudo-hexagonal prismatic shape with HCMS structure as the parent carbon nanocases, still preserving the shape of the silicalite-1 crystals even after repeated replications. Unlike working with amorphous solid core and mesoporous shell spheres in previous work,<sup>12</sup> extra care was taken in handling silicalite-1 zeolite and ZCMS particles because they tend to easily aggregate in solution. If this would happen, the carbon and silica nanocases might be glued together to become big chunks by contact mainly through their wide flat surfaces. Care has been exercised by sonication at ambient temperature in solution and also by relatively strong stirring to set the particles as far apart as possible during reaction. It is also particularly important to introduce the proper amount of precursor solution into the template in order to have clean replication products by means of careful processing and treatment including the use of vapor phase precursor, infiltration under static vacuum condition, removal of excess by vacuum evaporation, and controlled oligomerization reactions in specific sites of template framework in the case of liquid precursor. Interestingly, the silica nanocases look more transparent compared to the carbon nanocases in the SEM images. After all, such subsequent replications also resulted in the first synthesis of the nonspherical uniform monodisperse nanocases with HCMS structures made of carbon and silica. The shell thickness of the HCMS carbon and silica nanocases determined from the TEM images was about 35 nm for both cases. They also showed three-dimensionally interconnected randomly disordered pore arrangements in the shell. Each of the nanocases has a hierarchical pore structure with a hollow macroporous core and mesoporous shell, and thus is lightweight, which is favorable for applications. These nonspherical hollow nanocases with flat surfaces can be utilized as nanoblocks for various self-assembly processes.<sup>23</sup>

The mechanical strength of the hollow nanocases was roughly examined by monitoring their SEM images after pressurizing pelletized carbon and silica nanocase disks (each 100 mg and 1/2 in. diameter) at different pressures for 10 min. There was no significant change at the low-pressure range less than 250 MPa, but about 70–85% nanocases became compressed to be platy particles after 650 MPa pressure for the carbon. However, silica showed much less mechanical stability. Silica showed not

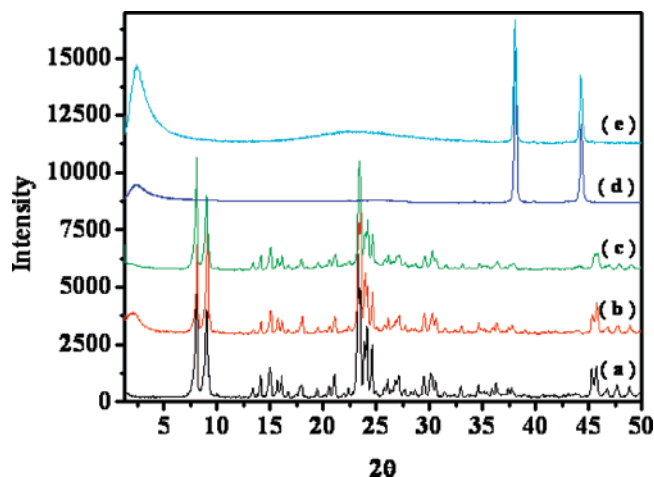


**Figure 3.** Powder X-ray diffraction (XRD) patterns for (a) calcined silicalite-1, (b) silicalite-1 ZCMS silicate, (c) carbon-ZCMS silicate template nanocomposite, (d) HCMS carbon nanocases, and (e) HCMS silica nanocases.

much change in the pressure range less than 150 MPa, but about 80–90% silica nanocases were compressed after 450 MPa.

Figure 3 shows the X-ray diffraction patterns of silicalite-1 core particles, ZCMS core–shell silicate particles, carbon–ZCMS silicate composites, and HCMS carbon and silica nanocases, respectively. The XRD pattern of silicalite-1 coincides with that reported in the literature.<sup>15,21</sup> The XRD pattern of the silicalite-1 ZCMS silicate particles (Figure 3b) shows an additional low-angle peak at  $2\theta = 1.5$ – $3.0$  due to the presence of the mesoporous shell in addition to the higher  $2\theta$  peaks due to silicalite-1 structure. In carbon–ZCMS silicate composite (Figure 3c), the XRD peak intensity due to silicalite-1 was almost the same, but the low-angle signal due to the mesoporous shell significantly decreased compared to that of the parent ZCMS template. This implies that the carbon has been embedded only in the mesoporous shells of the silicalite-1 ZCMS core–shell silicate templates, and little carbon is in the micropores of the silicalite-1 cores due to the narrow pore size of the micropores of silicalite-1. This is additional evidence that the carbon precursor predominantly enters only the mesopores in accordance with the TEM image shown in Figure 2a. Figure 3d and Figure 3e show XRD patterns of the HCMS carbon and silica, respectively. All the higher  $2\theta$  peaks due to the ordered silicalite-1 microporous structure have disappeared. This indicates a complete removal of the silicalite-1 core, showing a hollow core in the structure. This is also consistent with the TEM images of the carbon and silica nanocases with hollow cores. Two strong XRD peaks at  $2\theta = 38$  and  $44$ , respectively, are observed and are assigned to an aluminum sample holder for XRD measurements. Interestingly, these peaks are not observed for silicalite-1, ZCMS, and their composite materials with dense core structures. This observation further supports the fact that the carbon and silica nanocases actually have hollow cores. This indicates that X-rays can penetrate the hollow core nanocases, and their diffraction from the aluminum plate was collected at the detector. The two peaks were not observed when the same measurements were made with a glass sample holder. The low-angle signal assigned to the mesoporous shell regained intensity, but shifted slightly to a higher angle of  $2\theta = 2.0$ – $4.0$ , probably due to the shrinkage of the framework during the templated synthesis of these nanocase materials. In fact, the carbon and silica nanocases experienced shrinkage during replication by 8–13% and 12–18% as compared with the dimension of the zeolite crystal. A broad signal was observed

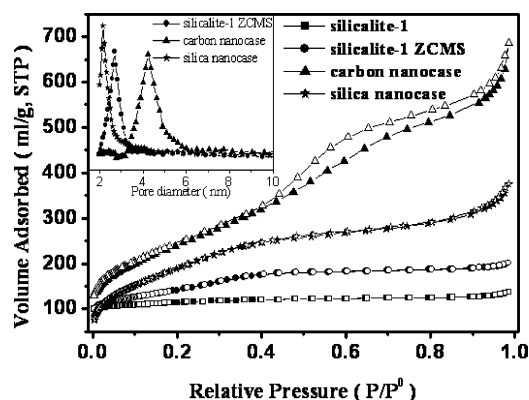


**Figure 4.**  $N_2$  adsorption/desorption isotherms for silicalite-1 (■), silicalite-1 ZCMS silicate particles (●), HCMS carbon nanocases (▲), and HCMS silica nanocases (★) and their corresponding pore size distribution curves (inset).

**TABLE 1: Structural Properties of Calcined Silicalite-1 Particles, Silicalite-1 ZCMS Silicate Particles, and HCMS Carbon and Silica Nanocases**

sample name	shell thickness <sup>a</sup> (nm)	BET surf. area (m <sup>2</sup> /g)	total pore vol (mL/g)	pore size <sup>b</sup> (nm)
silicalite-1		415	0.30	
silicalite-1 ZCMS	40	518	0.46	2.7
HCMS carbon	35	918	1.40	4.3
HCMS silica	35	726	0.86	2.2

<sup>a</sup> Shell thickness determined from the TEM images. <sup>b</sup> Maximum value of the BJH pore size distribution peak calculated from the adsorption branch of the  $N_2$  isotherm.

in the range of  $2\theta = 15$ – $30$  for the HCMS silica and is considered to be due to the presence of amorphous silica.

Typical nitrogen adsorption/desorption isotherms at 77 K for silicalite-1, ZCMS core–shell silicate, and HCMS carbon and silica nanocases, and their corresponding pore size distributions, are shown in Figure 4. The sorption isotherm for silicalite-1 particles indicates a characteristic of microporous materials with Langmuir type (type I); a rise at low relative pressure and then a pronounced plateau. Their total pore volume and surface area are lower compared with those of the ZCMS particles and carbon and silica nanocases. The ZCMS core–shell and carbon and silica nanocases all exhibit a type IV isotherm characteristic of mesoporous solids according to IUPAC nomenclature.<sup>17</sup> This again implies that they possess mesopores in the framework. Their corresponding pore size distribution data calculated from the adsorption branches of nitrogen isotherms by the BJH (Barrett–Joyner–Halenda) method showed that pores are uniform and centered at 2.7, 4.3, and 2.2 nm, respectively. The structural parameters for the synthesized materials are summarized in Table 1. It was possible to control of the shell thickness and the mesopore size of ZCMS core–shell particles mainly by monitoring the amount and ratio of TEOS and  $C_{18}$ -TMS added. The pore size increases with relative concentration of  $C_{18}$ -TMS, which has the function of a porogen to generate the porosity in the shell. The pore size increased to 3.4 nm with molar ratio of TEOS/ $C_{18}$ -TMS = 3.5. However, the mesoporous shell was poorly formed or not generated over ZSM-5 core crystals at the molar ratio of 3.0 or lower.

After all, the silicalite-1 ZCMS core–shell silicate particles have pseudohexagonal prismatic shapes and hierarchical porous frameworks of microporous silicalite-1 core and mesoporous shell structures with even shell thickness and uniform pore size. Carbon and silica nanocases each also have a bimodal pore

system composed of a nonspherical pseudohexagonal prismatic macroporous core and mesoporous shell.

## Conclusions

In this work, the synthesis of hierarchical porous core–shell silicate particles consisting of silicalite-1 zeolite crystal cores and mesoporous shells was demonstrated for the first time. The ZCMS core–shell particles represent unique and novel structures in that they have pseudohexagonal prismatic shape and bimodal porosity of both uniform micropores and mesopores coexisting in a particle framework. The control of the shell thickness and mesopore size is possible by monitoring the amount and ratio of TEOS and  $C_{18}$ -TMS added and thermal treatment. New nonspherical carbon nanocases with HCMS structure were fabricated using the porous ZCMS particles as templates. The mesoporous carbon structures also provide an opportunity for generation of various novel nanostructured inorganic materials, which otherwise are not possible to synthesize through other synthetic methods. As an example in this work, new pseudohexagonal prismatic silica nanocases were fabricated by replication using the carbon nanocases as templates and TEOS as a silica source. Since there are various shapes of zeolite crystals available, the preparation of various types of zeolite core-containing core–shell silicates and corresponding HCMS nanocase materials with different shapes and compositions can be possible by using the zeolite crystals as templates and different precursors as component materials. The hierarchically nanoporous ZCMS core–shell silicates and carbon and oxide ceramic nanocases with HCMS structures can find a wide range of potential applications such as catalysts, in chromatography, as adsorbents, as electrode materials, as storage materials, and as nanoblocks for self-assembly processes.

**Acknowledgment.** The authors thank the Hannam University for financial support and the Korean Basic Science Institution for TEM and SEM analyses.

## References and Notes

- (1) (a) Breck, D. W. *Zeolite Molecular Sieves: structure, chemistry, and use*; John Wiley & Sons: New York, 1974; Chapter 1. (b) Corma, A. *Chem. Rev.* **1997**, *97*, 2373. (c) Zhao, D.; Feng, J.; Huo, Q.; Melosh, N.; Fredrickson, G. H.; Chmelka, B. F.; Stucky, G. D. *Science* **1998**, *279*, 548.
- (2) (a) Kyotani, T.; Ma, Z.; Tomita, A. *Carbon* **2003**, *41*, 1451. (b) Ma, Z.; Kyotani, T.; Tomita, A. *Carbon* **2002**, *40*, 2367. (c) Meyers, C. J.; Shah, S. D.; Patel, S. C.; Sneeringer, R. M.; Bessel, C. A.; Dollahon, N. R.; Leising, A. R.; Takeuchi, E. S. *J. Phys. Chem. B* **2001**, *105*, 2143. (d) Rodriguez-Mirasol, J.; Cordero, T.; Radovic, L. R.; Rodriguez, J. J. *Chem. Mater.* **1998**, *10*, 550. (e) Johnson, S. A.; Brigham, E. S.; Ollivier, P. J.; Mallouk, T. E. *Chem. Mater.* **1997**, *9*, 2448.
- (3) (a) Yoon, S. B.; Kim, J. Y.; Yu, J.-S. *Chem. Commun.* **2002**, 1536. (b) Kim, J. Y.; Yoon, S. B.; Kooli, F.; Yu, J.-S. *J. Mater. Chem.* **2001**, *11*, 2912. (c) Ryoo, R.; Joo, S. H.; Jun, S. J. *Phys. Chem. B* **1999**, *103*, 7743. (d) Lee, J.; Yoon, S.; Hyeon, T.; Oh, S. M.; Kim, K. B. *Chem. Commun.* **1999**, 2177. (e) Yang, H.; Shi, Q.; Liu, X.; Xie, S.; Jiang, D.; Zhang, F.; Yu, C.; Tu, B.; Zhao, D. *Chem. Commun.* **2002**, 2842. (f) Vix-Guterl, C.; Boulard, S.; Parmentier, J.; Werckmann, J.; Patarin, J. *Chem. Lett.* **2002**, *31*, 1062.
- (4) (a) Lu, A.; Kiefer, A.; Schmidt, W.; Schuth, F. *Chem. Mater.* **2004**, *16*, 100. (b) Yoon, S. B.; Kim, J. Y.; Yu, J.-S. *Chem. Commun.* **2003**, 1740. (c) Kim, S.-S.; Lee, D.-K.; Shah, J.; Pinnavaia, T. J. *Chem. Commun.* **2003**, 1436. (d) Vinu, A.; Streb, C.; Murugesan, V.; Hartman, M. J. *Phys. Chem. B* **2003**, *107*, 8297. (e) Zhang, W.-H.; Liang, C.; Sun, H.; Shen, Z.; Guan, Y.; Ying, P.; Li, C. *Adv. Mater.* **2002**, *14*, 1776. (f) Joo, S. H.; Choi, S. J.; Oh, I.; Kwak, J.; Liu, Z.; Terasaki, O.; Ryoo, R. *Nature* **2001**, *412*, 169. (g) Jun, S.; Joo, S. H.; Ryoo, R.; Kruk, M.; Jaroniec, M.; Liu, Z.; Ohsuna, T.; Terasaki, O. *J. Am. Chem. Soc.* **2000**, *122*, 10712.
- (5) (a) Jiang, P.; Bertone, J. F.; Colvin, V. L. *Science* **2001**, *291*, 453. (b) Johnson, S. A.; Ollivier, P. J.; Mallouk, T. E. *Science* **1999**, *283*, 963.
- (6) (a) Holland, B. T.; Blanford, C. F.; Do, T.; Stein, A. *Chem. Mater.* **1999**, *11*, 795. (b) Velev, O. D.; Jede, T. A.; Lobo, R. F.; Lenhoff, A. M. *Chem. Mater.* **1998**, *10*, 3597. (c) Park, S. H.; Xia, Y. *Adv. Mater.* **1998**,

- 10, 1045. (d) Imhof, A.; Pine, D. J. *Adv. Mater.* **1998**, *10*, 697. (e) Jiang, P.; Cizeron, J.; Bertone, J. F.; Colvin, V. L. *J. Am. Chem. Soc.* **1999**, *121*, 7957.
- (7) (a) Yan, H. W.; Blanford, C. F.; Holland, B. T.; Parent, M.; Smyrl, W. H.; Stein, A. *Adv. Mater.* **1999**, *11*, 1003. (b) Egan, G. L.; Yu, J.-S.; Kim, C. H.; Lee, S. J.; Schaak, R. E.; Mallouk, T. E. *Adv. Mater.* **2000**, *12*, 1040.
- (8) (a) Chai, G.; Yoon, S. B.; Yu, J.-S.; Choi, J.-H.; Sung, Y.-E. *J. Phys. Chem. B* **2004**, *108*, 7074. (b) Gierszal, K. P.; Jaroniec, M. *Chem. Commun.* **2004**, 2576. (c) Yu, J.-S.; Kang, S.; Yoon, S. B.; Chai, G. *J. Am. Chem. Soc.* **2002**, *124*, 9382. (d) Li, Z.; Jaroniec, M. *J. Am. Chem. Soc.* **2001**, *123*, 9208. (e) Gundiah, G.; Govindaraj, A. A.; Rao, C. N. R. *Mater. Res. Bull.* **2001**, *36*, 1751. (f) Lei, Z.; Zhang, Y.; Wang, H.; Ke, Y.; Li, J.; Li, F.; Xing, J. *J. Mater. Chem.* **2001**, *11*, 1975. (g) Zakhidov, A. A.; Boughman, R. H.; Iqbal, Z.; Cui, C. X.; Khayrullin, I.; Danta, S. O.; Marti, L.; Ralchenko, V. G. *Science* **1998**, *282*, 897.
- (9) (a) Sung, I. K.; Yoon, S. B.; Yu, J.-S.; Kim, D.-P. *Chem. Commun.* **2002**, 1480. (b) Wang, H.; Yu, J.-S.; Li, X.-D.; Kim, D.-P. *Chem. Commun.* **2004**, 2352.
- (10) (a) Buchel, G.; Unger, K. K.; Matsumoto, K.; Tsutsumi, K. *Adv. Mater.* **1998**, *10*, 1036. (b) Graft, C.; Vossen, D. L. J.; Imhof, A.; van Blaaderen, A. *Langmuir* **2003**, *19*, 6693. (c) Valtchev, V. *Chem. Mater.* **2002**, *14*, 956. (d) Zhu, G.; Qiu, S.; Terasaki, O.; Wei, Y. *J. Am. Chem. Soc.* **2001**, *123*, 7723. (e) Dong, A.; Wang, Y.; Tang, Y.; Ren, N.; Zhang, Y.; Gao, Z. *Chem. Mater.* **2002**, *14*, 3217. (f) Ohmori, M.; Matijevic, E. *J. Colloid Interface Sci.* **1993**, *160*, 288.
- (11) (a) Marinakos, S. M.; Novak, J. P.; Brousseau, L. C., III; House, A. B.; Edeki, E. M.; Feldhaus, J. C.; Feldheim, D. L. *J. Am. Chem. Soc.* **1999**, *121*, 8518. (b) Yu, J.-S.; Kim, J. Y.; Lee, S.; Mbindyo, J. K. N.; Martin, B. R.; Mallouk, T. E. *Chem. Commun.* **2000**, 2445. (c) Dahne, L.; Leporatti, S.; Donath, E.; Mohwald, H. *J. Am. Chem. Soc.* **2001**, *123*, 5431. (d) Caruso, F.; Spasova, M.; Susha, A.; Giersig, M.; Caruso, R. A. *Chem. Mater.* **2001**, *13*, 109. (e) Kamata, K.; Lu, Y.; Xia, Y. *J. Am. Chem. Soc.* **2003**, *125*, 2384. (f) Caruso, F. *Chem. Eur. J.* **2000**, *6*, 413.
- (12) Yoon, S. B.; Sohn, K.; Kim, J. Y.; Shin, C. H.; Yu, J.-S.; Hyeon, T. *Adv. Mater.* **2002**, *14*, 19. (b) Kim, M.; Yoon, S. B.; Sohn, K.; Kim, J. Y.; Shin, C.-H.; Hyeon, T.; Yu, J.-S. *Microporous Mesoporous Mater.* **2003**, *63*, 1.
- (13) (a) Caruso, F. *Adv. Mater.* **2001**, *13*, 11. (b) Dai, Z.; Dahne, L.; Mohwald, H.; Tiersch, B. *Angew. Chem., Int. Ed.* **2002**, *41*, 4019 and references therein.
- (14) Occelli, M. L.; Robson, H. E. *Zeolite Synthesis*; American Chemical Society: Washington, DC, 1989.
- (15) (a) Zhu, G.; Qui, S.; Yu, J.; Sakamoto, Y.; Xiao, F.; Xu, R.; Terasaki, O. *Chem. Mater.* **1998**, *10*, 1483. (b) U.S. Patent 3,702,886, 1972. (c) U.S. Patent 4,061,724, 1977.
- (16) Kim, J. Y.; Lee, S. J.; Yu, J.-S. *Bull. Korean Chem. Soc.* **2000**, *21*, 544.
- (17) Sing, K. S. W.; Everett, D. H.; Haul, R. A. W.; Moscou, L.; Pierotti, R. A.; Rouquerol, J.; Siemieniewska, T. *Pure Appl. Chem.* **1985**, *57*, 603.
- (18) (a) Holland, B. T.; Abrams, L.; Stein, A. *J. Am. Chem. Soc.* **1999**, *121*, 4308. (b) Lebeau, C.; Fowler, E.; Mann, S.; Farcet, C.; Charleux, B.; Sanchez, C. *J. Mater. Chem.* **2000**, *10*, 2105.
- (19) van Koningsveld, H.; van Nekkum, H.; Jansen, J. C. *Acta Crystallogr.* **1987**, *B43*, 127.
- (20) Breck, D. W. *Zeolite Molecular Sieves: structure, chemistry, and use*; John Wiley & Sons: New York, 1974; Chapter 8.
- (21) Anderson, M. W.; Kevan, L. *J. Phys. Chem.* **1987**, *91*, 4147.
- (22) (a) Kang, M.; Yi, S. H.; Lee, H. I.; Yie, J. E.; Kim, J. M. *Chem. Commun.* **2002**, 1944. (b) Lu, A.-H.; Schmidt, W.; Taguchi, A.; Spliethoff, B.; Tesche, B.; Schuth, F. *Angew. Chem., Int. Ed.* **2002**, *41*, 3489. (c) Yoon, S. B.; Kim, J. Y.; Yu, J.-S. *Chem. Mater.* **2003**, *15*, 1932.
- (23) (a) Katagiri, K.; Hamasaki, R.; Ariga, K.; Kikuchi, J.-I. *J. Am. Chem. Soc.* **2002**, *124*, 7892. (b) Ariga, K. *Chem. Record* **2004**, *3*, 297. (c) Caruso, F.; Lichtenfeld, H.; Giersig, M.; Mohwald, H. *J. Am. Chem. Soc.* **1998**, *120*, 8523.